ELSEVIER

Biochimica et Biophysica Acta 1329 (1997) 245–258

BIOCHIMICA ET BIOPHYSICA ACTA
BBA

Interaction of a highly potent dimeric enkephalin analog, biphalin, with model membranes

Marek Romanowski, Xiaoyun Zhu, Varadarajan Ramaswami, Aleksandra Misicka, Andrzej W. Lipkowski, Victor J. Hruby, David F. O'Brien *

Department of Chemistry, University of Arizona, P.O. Box 210041, Tucson, AZ 85721, USA

Received 30 January 1997; revised 30 April 1997; accepted 1 May 1997

Abstract

Biphalin, (Tyr–D-Ala–Gly–Phe–NH)$_2$, is a highly potent dimeric analog of enkephalin. Its analgesic efficacy is due in part to its ability to permeate the blood–brain barrier. To aid in understanding the mechanism of the transmembrane movement we determined and analyzed the permeability and partition coefficients of biphalin and a series of analogues where F, Cl, I, NO_2, or NH_2 were placed in the *para* position of the aromatic rings of Phe$^{4,4'}$. Liposomes composed of neutral phospholipids and cholesterol were used as the model membrane. The overall good correlation between permeability and water-membrane partition coefficients suggests that the movement of biphalins across the model membrane is controlled by diffusion and depends on the water-membrane partition coefficient. To explain the observed correlation between permeability and the electron withdrawing/donating character of the substituents in the phenylalanine ring, we examined various folding patterns of Leu–enkephalin, an endogenous pentapeptide that exhibits affinities toward the same classes of opioid receptors (δ and μ). The observed permeabilities and partition coefficients of biphalin and analogues, as well as the tyrosine side chain accessibility, are consistent with the presence of the type of folding where the tyrosine and phenylalanine side chains are in a close contact. We propose that the aromatic ring interaction can promote the peptide permeability by stabilizing a more compact structure of biphalin that would minimize the number of hydrogen bonds with water and therefore enhances partitioning into the model membrane. © 1997 Elsevier Science B.V.

Keywords: Opioid peptide; Drug design; Blood-brain barrier; Permeability; Partitioning; Lipid membrane

1. Introduction

A major question of importance to medicine, pharmacology, cell biology, and biological chemistry is the nature of diffusion and transport of molecular species across cell membranes. Concepts of membrane transport and diffusion have evolved with the increased understanding of the structure of cell membranes (see monographs [1,2]). The movement of species across the membrane is accomplished either by passive diffusion across the membrane or by some

Abbreviations: DPPC, 1,2-dipalmitoylphosphatidylcholine; POPC, 1-palmitoyl-2-oleoylphosphatidylcholine; POPE, 1-palmitoyl-2-oleoylphosphatidylethanolamine; biphalin, (Tyr–D-Ala–Gly–Phe–NH)$_2$; DSC, differential scanning calorimetry; T_m, gel to liquid-crystalline phase transition temperature (measured as the temperature at the maximum of excess heat capacity); ΔH_{cal}, calorimetric enthalpy of the lipid phase transition; ΔH_{vH}, Van't Hoff enthalpy of the lipid phase transition; CU, size of the cooperative unit (calculated as $CU = \Delta H_{vH}/\Delta H_{cal}$); P, permeability coefficient; K, water–membrane partition coefficient of peptides

* Corresponding author. Fax: +1-520-6218407.

PII S0005-2736(97)00115-6

facilitated transport process, which may be associated with a membrane protein or a smaller transport molecule. Although mediated transport processes are especially important to the natural functioning of the cell, these transport processes are frequently not available for the membrane movement of added pharmacological agents. Thus, diffusion is the primary process of membrane translocation for many therapeutic agents from the blood stream into various regions of the body including the brain.

According to the diffusion model for membrane transport, permeability coefficients are related to the product of the water–membrane partition coefficient of the permeant and the normal component of the diffusion coefficient [3]. The coefficient of partition between polar and bulk nonpolar phases is a foundation of the hydrophobicity scale of amino acids [4]. Conveniently, this hydrophobicity scale can be related to the accessible surface area of the given amino acid residue [5]. If one takes into account corrections for possible hydrogen bond formation between polar residues and water, a linear relation between accessible surface area and hydrophobicity is obtained and may be expressed as a molar energy of transfer from water to the nonpolar solvent [5]. On the other hand, the diffusional properties of the membrane are strongly heterogeneous. At least two distinct regions can be identified, the highly polar interface and the hydrocarbon interior [3]. Unlike a bulk solvent, permeabilities in biological membranes and model bilayers depend strongly on the volume of the diffusing molecule [1,6].

Detailed analysis of the peptide partitioning between water and lipid bilayers reveals the complexities of this phenomenon. There are several effects that contribute to the partitioning of the peptide molecule between water and the lipid bilayer. Besides the aforementioned hydrophobic effect there is the peptide immobilization effect, conformational changes of peptides, intermolecular hydrogen bonds, membrane lateral pressure and lipid perturbation, which generally oppose the transfer of peptides from aqueous to lipid phase [7–9]. The overall character of the peptide transfer process (e.g., endothermic or exothermic) is determined by the subtle interplay of all the contributing effects. All of those specificities of the partitioning and interfacial interactions lead to the conclusion that bulk-phase measurements are inadequate for describing bilayer partitioning [10]. Understanding of the mechanism of the transmembrane movement has practical significance, because the permeability of biological membranes that constitute the blood–brain barrier is a major obstacle in peptidic drug delivery to the brain [11]. Since the requirements for biological activity and permeability are not necessarily convergent, this creates an additional challenge for the development of peptidic drugs.

Here we describe studies of the permeation of the octapeptide biphalin across model membranes. Biphalin [(Tyr–D-Ala–Gly–Phe–$NH)_2$] is a most potent analgesic enkephalin analogue and in fact is more potent than most alkaloid opiates [12–14]. The affinity of this highly flexible peptide toward δ- and μ-opioid receptors can be partially controlled by various substitutions in the *para* position of $Phe^{4,4'}$ [14]. The efficacy of this analgesic relative to other peptides is improved due in part to its modest permeability of the blood–brain barrier [11,13,15]. In order to analyze the permeability and partitioning of biphalins, we have used a model membrane composed of neutral phospholipids and cholesterol, representing the major lipid components of vasculature membranes. The goal is to correlate the permeation and partition coefficients of the peptides with the *para*-substituent on the biphalins.

2. Materials and methods

2.1. Materials

The following lipids: 1,2-dipalmitoylphosphatidylcholine (DPPC), 1-palmitoyl-2-oleoylphosphatidylcholine (POPC) and 1-palmitoyl-2-oleoylphosphatidylethanolamine (POPE), were purchased from Avanti Polar Lipids, Alabaster, AL. Hepes and Hepps were purchased from Calbiochem, La Jolla, CA, sodium azide and sodium chloride from Aldrich, Milwaukee, WI, cholesterol and Triton TX-100 from Sigma, St. Louis, MO. Degassed Hepes buffer (10 mM Hepes, 150 mM sodium chloride, 1 mM sodium azide, 0.1 mM EDTA, pH 7.4) or Hepps buffer (10 mM Hepps, 150 mM sodium chloride, 1 mM sodium azide, 0.1 mM EDTA, pH 8.9) was used throughout the experiments. Dialysis membranes were purchased from Spectrum, Houston, TX. Leu–en-

kephalin (Tyr–Gly–Gly–Phe–Leu) and Tyr–D-Ala–Gly were purchased from Bachem, Torrance, CA, whereas biphalin (Tyr–D-Ala–Gly–Phe–$NH)_2$ and its analogues, were synthesized as described elsewhere [12].

2.2. Permeability assay

Following the method developed in our laboratory [16], 20 mg of a dried mixture of lipids and cholesterol was hydrated in 1 ml of Hepps buffer (pH 8.9) and sonicated to form homogenous suspension. The desired peptide was added and the mixture was vigorously stirred, frozen and thawed to form extended bilayers, which were then extruded at 40°C through polycarbonate filters with a pore size of 200 nm [17]. Liposomes, with trapped peptides, were separated from untrapped peptides by size exclusion chromatography on a Sephacryl S-300 column. A 2 ml fraction of liposome suspension was placed in a dialysis membrane bag and the pH was adjusted to 7.4. The dialysis system was designed specifically for this assay. A sample placed in the dialysis bag is dialyzed against 200 ml of buffer. The dialyzate is continuously pumped at the flow rate of 1.2 ml h^{-1} and the sample collected in 1.2 ml fractions by an automatic fraction collector. To assure the stability of the experimental conditions, the ambient temperature is thermostated at 25°C and the dialyzate is continuously stirred. All parts of the dialysis system are made of poly(methyl methacrylate) to minimize adsorption of peptides on its surfaces. The amount of peptide molecules released form liposomes into the dialyzate was determined by a fluorescamine assay [18]. The intensity of fluorescence excited at 380 nm and measured at 480 nm was used to quantify the peptide concentration. The permeability data were analyzed by the procedure of Johnson and Bangham [19] which yields the following equation

$$\ln\left[\frac{NV_{out}}{V_{in}+V_{out}}-N(t)\right]=\ln\frac{NV_{out}}{V_{in}+V_{out}}-k\frac{V_{out}+V_{in}}{V_{out}}t \quad (1)$$

where $N(t)$ is the number of peptide molecules in dialyzate at given time, N is the number of peptide molecules in liposomes at $t=0$, V_{out} is the volume of the dialyzate, V_{in} is the volume of the liposome suspension contained in the dialysis bag, finally $k=(A/V)P$, where A is the surface area of the inside liposomes, V is the internal volume of the liposomes and P is the permeability coefficient.

To estimate the number of peptide molecules initially trapped in the liposomes, we applied the following procedure. First, the liposomes were sized by dynamic light scattering, as described previously [16,20]. The apparent liposome diameter with entrapped peptides varied between 146 and 155 nm. The lipid content was determined by the ammonium ferrothiocyanate assay [21], as described in detail elsewhere [22]. The liposome diameter together with the lipid amount were used to calculate the total liposome volume. Finally, the peptide concentration inside the liposomes was assumed to be equal to the initial concentration of peptides in the lipid suspension before extrusion, which leads to the trapped amount of peptide, N. Eq. (1) represents a linear function of t, which allows for a calculation of the permeability coefficient, P, by the method of least squares. An alternative method was evaluated for determining the number of peptide molecules initially trapped in the liposomes, i.e., Triton X-100 lysis of the liposomes followed by the fluorescamine assay of the released peptides. However, the presence of Triton X-100 strongly affects the intensity of the fluorescamine–biphalin complex fluorescence. The presence of the detergent perturbs the N-termini accessi-

Table 1
Permeability and partition coefficients

Peptide	Permeability coefficient (10^{-12} cm s^{-1})	Partition coefficient
[*p*-F-$Phe^{4,4'}$]-biphalin	2.58 ± 0.67	2188 ± 324
[*p*-I-$Phe^{4,4'}$]-biphalin	1.05 ± 0.21	ND
[*p*-Cl-$Phe^{4,4'}$]-biphalin	1.01 ± 0.12	1460 ± 38
biphalin	0.68 ± 0.15	861 ± 121
[*p*-NO_2-$Phe^{4,4'}$]-biphalin	0.29 ± 0.02	<100
[*p*-NH_2-$Phe^{4,4'}$]-biphalin	0.22 ± 0.02	130 ± 52
Leu–enkephalin	3.80 ± 0.46	ND

Liposomes composed of POPC:POPE:cholesterol at the molar ratio 65:25:10 served as a model membrane. Concentration of peptides was determined by intensity of the intrinsic fluorescence due to tyrosine (for the partition coefficient determination) or by extrinsic fluorescent probe, fluorescamine (for the permeability coefficient).
ND: not determined.

bility to interactions with fluorescamine, preventing quantitative analysis by this assay.

The above method is not corrected for the biphalin peptide that resides in the lipid phase. The partition coefficient, K, can be used to calculate the molar concentration of peptides in the membrane, C_m^p, and aqueous phase C_a^p where $C_a^p = C_{tot}^p - C_m^p$, and C_m' is the molar concentration of lipids and C_a^w is the water concentration. Using the relationship

$$C_a^p = C_{tot}^p \frac{1}{1 + K\left(C_m'/C_a^w\right)} \quad (2)$$

it can be shown that for a K of 10^3, the value of C_a^p is $5/6$ of the original C_{tot}^p, and for a K value of 10^2, the C_a^p value is $50/51$ of C_{tot}^p. These errors are similar or less than the uncertainties cited in Table 1.

2.3. Equilibrium dialysis

We have developed an equilibrium dialysis assay to determine partitioning of the opioid peptides between the aqueous phase and model membranes. Each dialysis cell is separated by a cellulose dialysis membrane, average MW cut off 12 000–14 000. 1 ml of ca. 0.1 mM peptide solution in buffer is placed on the *cis* side of the membrane, whereas 1 ml of a lipid suspension in the same buffer is placed on the *trans* side. In the experiments performed, the five cells contained 40, 30, 20, 10 and 0 mM lipid suspension. Samples were equilibrated overnight in a water bath, using five cells mounted in a rotor that ensures homogeneity of peptide and lipid distribution in the dialysis cells. After the equilibration time, the concentrations of peptides on the *cis* side (therefore unbound) were determined by measurements of the intrinsic peptide fluorescence (all peptides under study contain tyrosine). Data were analyzed using a nonsaturable partitioning model, which yields the partition coefficient:

$$\frac{I_0}{I} = \frac{K[\mathrm{L}]}{2[\mathrm{W}]} + 1 \quad (3)$$

where I is the intensity of fluorescence, I_0 is the intensity of fluorescence in the cell with no lipids on the *trans* side, [L] is the concentration of lipids in the *trans* compartment, [W] is the concentration of water, K is the partition coefficient, and factor 2 is to correct the lipid concentration for the doubled volume accessible to the peptides, i.e., the *cis* and *trans* compartment volume, rather than *trans* only. The total volume of the sample was taken into consideration. At equilibrium both the interior and exterior aqueous compartments are equivalent. The volume of the lipids was not subtracted, since it is less than 2% of the total. This method does not limit the lipid system used in the experiments, therefore it is possible to use the same lipid composition as that used in the permeability experiments. The lipid suspension was prepared following the method described in Section 2.2, except no peptide was added to the suspension.

2.4. Differential scanning calorimetry

Peptide molecules penetrating a membrane perturb the lipid order of the membrane. The extent of this perturbation can be determined by measuring the heat capacity profile of the lipid phase transition. Hence differential scanning calorimetry (DSC) is a convenient tool for characterizing peptide-membrane interactions. Preparation of the lipid suspensions and calorimetric measurements were performed in a similar manner as described by Ramaswami et al. [16]. Multilamellar lipid suspensions were prepared from 1 mg DPPC hydrated with 1 ml of Hepes buffer (pH 7.4). A desired amount of a peptide was added and suspension was mixed and incubated at 41.5°C for ca. 12 h. Calorimetric measurements were performed immediately after the sample incubation. The measurements were repeated at different (decreasing) concentrations of peptides. These concentrations were adjusted by adding aliquots of the lipid suspension, and sample was again mixed and incubated for ca. 12 h prior to the measurement. To monitor the possibility of hydrolysis of the DPPC, the sample was analyzed by thin layer chromatography (TLC). The eluent was a mixture of chloroform:methanol:water (65:25:4) and the TLC plate was stained by phosphomolybdic acid. Only one spot was detected over the duration of the experiment.

DSC measurements were performed with a Microcal MC-2 scanning calorimeter (Microcal, Northampton, MA) interfaced to a 486 PC computer. Both sample and reference (buffer) cells were pressurized

(40 psi, nitrogen) and heated at a constant rate of 10 deg h^{-1}. Collected thermograms were normalized and baseline was subtracted to obtain excess heat capacity curves. Analysis of these curves yields the temperature at the maximum of excess heat capacity, T_m, calorimetric enthalpy, ΔH_{cal}, and van't Hoff enthalpy, ΔH_{vH}. The size of cooperative unit, CU, was calculated as a ratio of the van't Hoff enthalpy to the calorimetric enthalpy.

2.5. Spectroscopic assays

The iodide (I^-) quencher stock solution was prepared as a 2 M KI solution with 1 mM $Na_2S_2O_3$, added to prevent formation of I_2, in the Hepes buffer, described above. The hypophosphate (HPO_4^{2-}) quencher was prepared as a 1 M Na_2HPO_4 solution in the Hepes buffer. The final pH value of these solutions was adjusted to pH 7.4 using NaOH or HCl as needed. The quenching experiment was performed in a 4 ml cuvette using a 0.1 mM or less concentrated peptide solution. The quencher stock solution was added to obtain the quencher concentrations between 10 and 200 mM. Fluorescence of the peptide due to tyrosine was excited at 275 nm and intensity at 305 nm was recorded as a function of the quencher concentration. The data were analyzed using the Stern–Volmer equation,

$$\frac{I}{I_0} = K_D[Q] + 1 \quad (4)$$

where: I is the fluorescence intensity, I_0 is the fluorescence intensity in the absence of the quencher, [Q] is the quencher concentration, and K_D is the Stern–Volmer quenching constant. Fluorescence intensities were corrected for the dilution due to the added quencher. The linear correlation coefficient was calculated to evaluate linearity of the data. All fluorescence spectra were recorded using a Spex Fluorolog spectrofluorometer.

Spectrophotometric titrations were performed as follows. Unbuffered ca. 0.1 mM solution of a peptide was used. The pH of the solution was varied by adding NaOH. Total dilution of the sample due to the base added did not exceed 5%. Absorption spectra were recorded using a Varian DMS-200 spectrophotometer. The absorbance at 290 nm as a function of pH was plotted and analyzed to obtain the pK_a. In both types of experiments, quenching and pH titration, biphalin, Leu–enkephalin, and Tyr–D-Ala–Gly, a non-functional control peptide corresponding to the N-terminal of biphalin, were compared.

3. Results

3.1. Permeability measurements

The lipids used in this study to prepare liposomes were a mixture of POPC, POPE and cholesterol in the molar ratio 65:25:10. The composition were selected as a reasonable first approximation to neutral lipid membranes. The palmitoyl and oleoyl chains were chosen to reflect the mix of *sn*-1 saturated and *sn*-2 unsaturated acyl chains. Published phase diagrams of saturated PC-cholesterol mixtures indicate that the lipid bilayer is in the liquid disordered phase when the cholesterol content is between 10 and 20 mol% and the temperature is at least 15°C above the main phase transition temperature (T_m) of the phospholipid [23,24]. Since the T_m values for POPC and POPE are below or near room temperature, respectively [25], and there is no evidence of a phase transition in the POPC:POPE:cholesterol mixture up to 60°C (DSC scans not shown), it is reasonable to expect that the model membrane used in these studies exist in the liquid disordered phase at the experimental temperature. The liposomes were prepared by extrusion (see Section 2) which yields predominantly unilamellar liposomes of uniform size and narrow polydispersity as shown by QELS and supported by negative stain electron microscopy [16]. Although some oligolamellar liposomes may be present, only the initial phase of the permeation, which is due to the outermost bilayer of the liposome, was used to calculate the permeability coefficient.

The permeability of the bilayer membranes to various solutes may be measured by dialysis of the liposome-entrapped solute provided that the rate of permeation through the dialysis bag is fast relative to the rate through the bilayer. The measured permeability coefficient for biphalins across the dialysis bag was ca. 10^{-4} cm s^{-1}, which is many orders of magnitude faster than the values measured when the

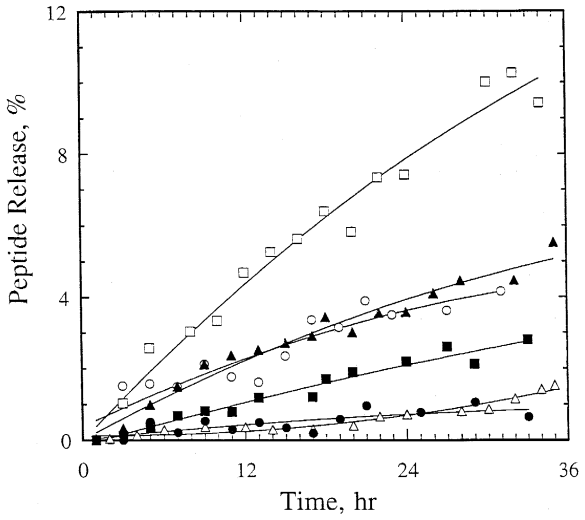

Fig. 1. Peptide release from phospholipid liposomes (POPC:POPE:cholesterol, 65:25:10) as determined by fluorescamine assay. Biphalin (■) and analogues: [*p*-F-Phe$^{4,4'}$]-biphalin (□), [*p*-I-Phe$^{4,4'}$]-biphalin (○), [*p*-Cl-Phe$^{4,4'}$]-biphalin (▲), [*p*-NO_2-Phe$^{4,4'}$]-biphalin (△) and [*p*-NH_2-Phe$^{4,4'}$]-biphalin (●).

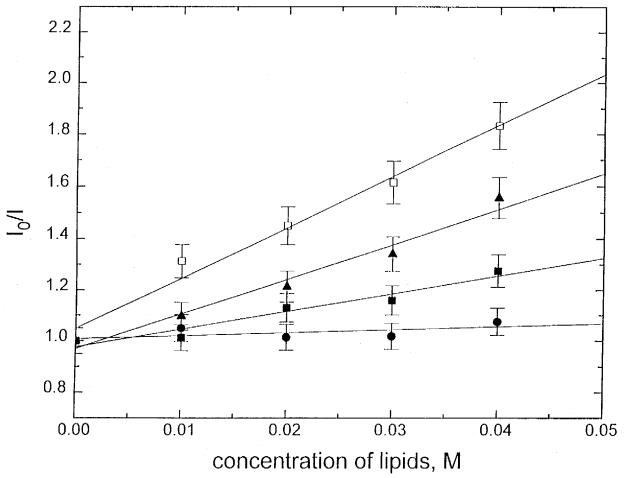

Fig. 2. Analysis of the equilibrium dialysis data. A 0.1 mM peptide solution was dialyzed against 0, 10, 20, 30 and 40 mM lipids in a form of liposomes. The peptide concentration in the aqueous phase after equilibration was determined by fluorescence. Biphalin (■) and selected analogues: [*p*-F-Phe$^{4,4'}$]-biphalin (□), [*p*-Cl-Phe$^{4,4'}$]-biphalin (▲), and [*p*-NH_2-Phe$^{4,4'}$]-biphalin (●). The slope of the reciprocal fluorescence intensity plotted as a function of the lipid concentration is proportional to the partition coefficient.

peptides were entrapped in liposomes inside the dialysis bag (see Table 1). Detection of the solute can be accomplished by radiochemical techniques, absorption and luminescence spectroscopy, as well as enzymatic or redox reactions. A convenient peptide assay is the rapid (millisecond) reaction of the free amino group with fluorescamine to yield highly fluorescent derivatives (excitation 380 nm, emission 475 nm). This assay is very sensitive with a reported detection limit of 50 pm for amino acids, and has been used to detect peptide hormones, e.g., vasopressin and oxytocin in individual rats, and opioids, e.g., β-endorphins [26]. Our calibration experiments with fluorescamine gave a detection limit of 2–5 nmol ml^{-1} for biphalin.

The profiles of permeation of the biphalin peptides studied (Table 1) through liposomes are shown in Fig. 1. Only a few percent of the peptides are released from the liposomes over several hours, which is much slower than the release from the dialysis membrane itself. The size exclusion chromatographic separation of the liposome entrapped peptide from the free peptide requires 30 to 45 min, during which time only a few tenths of a percent of the encapsulated peptide will escape the liposomes. Therefore, the fraction of peptides outside the liposomes but inside the dialysis bag is negligible at the start of the permeability experiment. The permeability coefficients of Leu–enkephalin and biphalins, modified by *p*-substituents on both phenylalanines, are reported in Table 1. In general, the halogenated biphalins are more permeable than the parent biphalin.

3.2. Equilibrium dialysis

The concentration of peptides prepared for this assay was optimized to assure a sufficient fluorescence intensity and, on the other hand, to prevent possible self-aggregation of peptides. The low solubility of [*p*-I-Phe$^{4,4'}$]-biphalin did not allow prepara-

Fig. 3. Thermograms for heating scans of biphalin: DPPC (a), *p*-Cl-Phe$^{4,4'}$-biphalin:DPPC (b), and *p*-NO_2-Phe$^{4,4'}$-biphalin:DPPC (c) mixtures. The molar ratio is given at the top of each panel. Values (averaged over three consecutive scans) of T_m, H_{cal}, H_{vH} and CU (symbols described in Section 2) are given in each panel. Thermograms shown were obtained with a 1.36 mM suspension of DPPC.

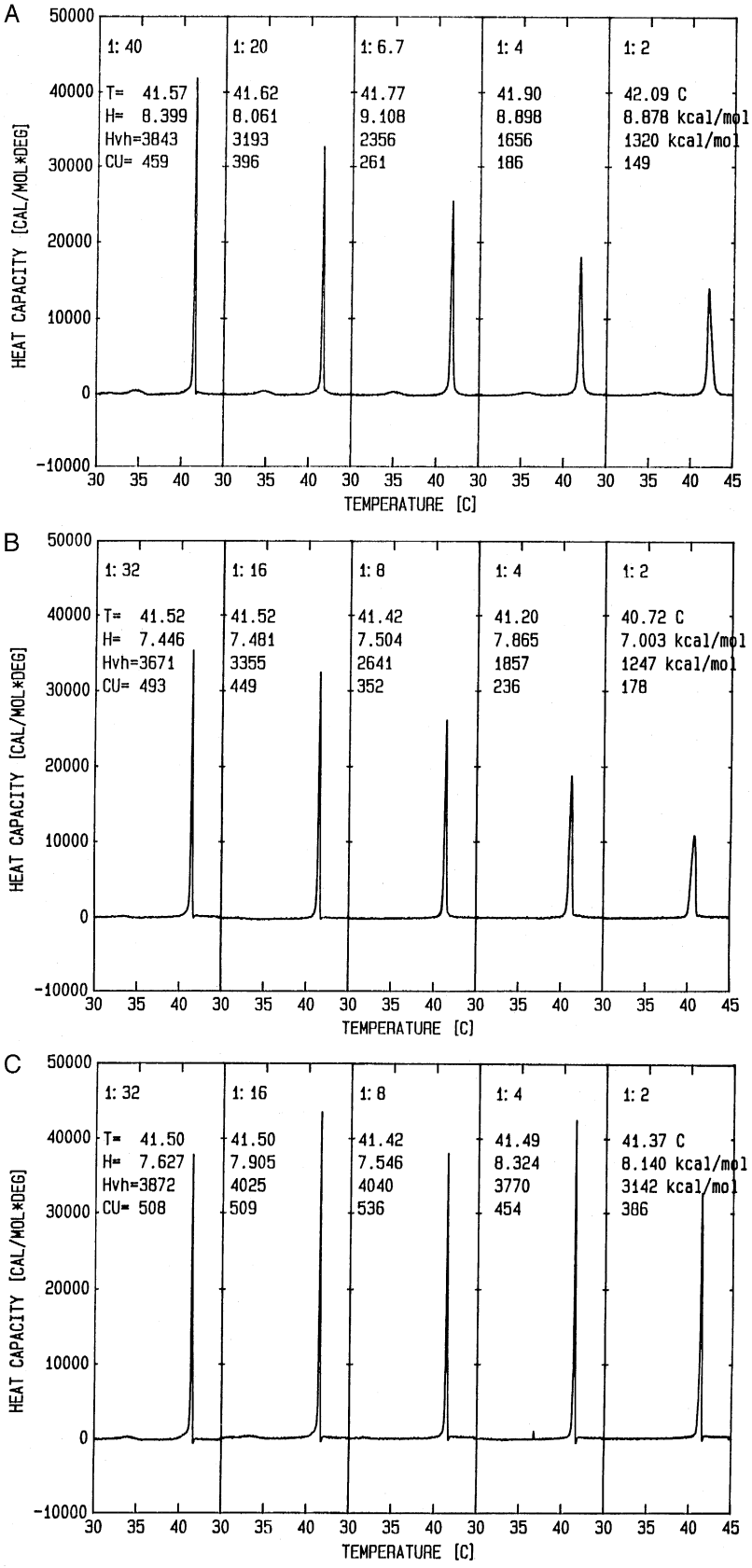
A
1: 40
T= 41.57
H= 8.399
Hvh=3843
CU= 459
1: 20
41.62
8.061
3193
396
1: 6.7
41.77
9.108
2356
261
1: 4
41.90
8.898
1656
186
1: 2
42.09 C
8.878 kcal/mol
1320 kcal/mol
149
HEAT CAPACITY [CAL/MOL*DEG]
TEMPERATURE [C]
B
1: 32
T= 41.52
H= 7.446
Hvh=3671
CU= 493
1: 16
41.52
7.481
3355
449
1: 8
41.42
7.504
2641
352
1: 4
41.20
7.865
1857
236
1: 2
40.72 C
7.003 kcal/mol
1247 kcal/mol
178
HEAT CAPACITY [CAL/MOL*DEG]
TEMPERATURE [C]
C
1: 32
T= 41.50
H= 7.627
Hvh=3872
CU= 508
1: 16
41.50
7.905
4025
509
1: 8
41.42
7.546
4040
536
1: 4
41.49
8.324
3770
454
1: 2
41.37 C
8.140 kcal/mol
3142 kcal/mol
386
HEAT CAPACITY [CAL/MOL*DEG]
TEMPERATURE [C]

tion of a sufficiently concentrated sample. The peptide concentration in the aqueous phase was analyzed by measuring the intensity of the intrinsic fluorescence of the peptides. Reciprocal fluorescence intensities are plotted as a function of the lipid concentration in the *trans* compartment (Fig. 2). The partition coefficient is proportional to the slope of this linear dependence, as described by Eq. (2). Partition coefficients of the halogenated analogues are higher than that of the parent compound, biphalin (Table 1). The [*p*-NH_2-Phe$^{4,4'}$]-biphalin analog shows very low partitioning, that approaches the detectability limit. Interestingly, the observed partition coefficients of the biphalins parallel the permeability measurements, indicating that the relative permeabilities of these peptides is dependent on biphalin partitioning.

The detection limit of this assay was determined as follows. Assuming the reproducibility of the fluorescence measurements to be 5% and considering the range of lipid concentration, 0 to 40 mM, the lowest value of the reproducibly detected partition coefficient is ca. 100. If the peptide studied here has the partition coefficient of this order of magnitude, i.e., *p*-NO_2-Phe$^{4,4'}$-biphalin, the measured partition coefficient was indicated as < 100 (Table 1).

3.3. Differential scanning calorimetry

The excess heat capacity curves for mixtures of DPPC with biphalin, [*p*-Cl-Phe$^{4,4'}$]-biphalin or [*p*-NO_2-Phe$^{4,4'}$]-biphalin are presented in Fig. 3. Increasing concentrations of these peptides induced distinctive changes in the thermodynamic properties. Biphalin increases the main transition temperature of DPPC (41.52°C for pure DPPC), whereas [*p*-Cl-Phe$^{4,4'}$]-biphalin and [*p*-NO_2-Phe$^{4,4'}$]-biphalin reduce this temperature. Even at the highest peptide-to-lipid molar ratio (1:2) these changes do not exceed 0.8°C. However perhaps the most obvious effect that accompanies the peptide–lipid interaction is the reduced size of the lipid cooperative unit at this concentration of peptides. The cooperative unit size is reduced to 149, 178 and 386 lipid molecules when interacting with biphalin, [*p*-Cl-Phe$^{4,4'}$]-biphalin or [*p*-NO_2-Phe$^{4,4'}$]-biphalin, respectively, as compared to ca. 600 for a pure phospholipid suspension. This results from a significant change of van't Hoff enthalpy rather than calorimetric enthalpy, which remains relatively constant. This behavior of the van't Hoff and calorimetric enthalpy indicates that the peptide upon entering the model membrane does not interact strongly with lipids and does not prevent individual lipid molecules from conformational rearrangements characteristic of cooperative membrane behavior. The increasing biphalin or [*p*-Cl-Phe$^{4,4'}$]-biphalin concentration decreases the excess heat capacity at the transition temperature, however this effect is not obvious for [*p*-NO_2-Phe$^{4,4'}$]-biphalin. Finally, it can be noted that the peptides which reduce the phase transition temperature, i.e., [*p*-Cl-Phe$^{4,4'}$]-biphalin and [*p*-NO_2-Phe$^{4,4'}$]-biphalin, efficiently remove the pretransition at 35°C (Fig. 3).

3.4. Spectroscopic assays

The pK_a values determined for the tyrosine hydroxyl groups of biphalin, Leu–enkephalin and the Tyr–D-Ala–Gly model peptide are identical within the experimental error (Fig. 4 and Table 2). The pK_a values determined for these peptides are within the range typical for solvent accessible tyrosine residues [27], and agree with the previous determination of pK_a for Leu–enkephalin [28]. Typically, it is prefer-

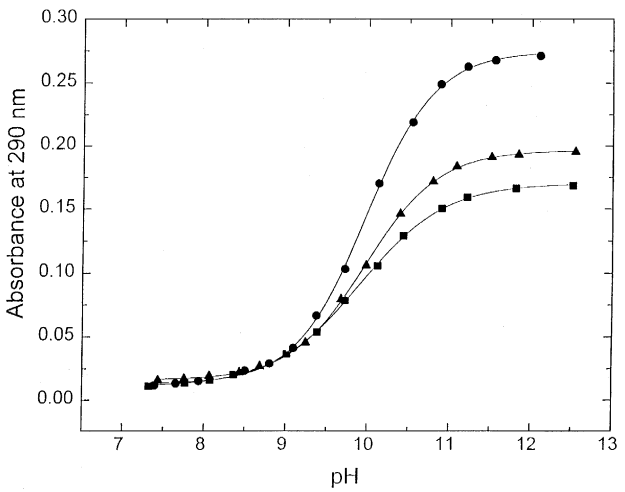

Fig. 4. Spectrophotometric titration curves of biphalin (■), Leu–enkephalin (▲) and Tyr–D-Ala–Gly (●). The curves represent absorbance at 290 nm, characteristic of the deprotonated form of tyrosine, as a function of pH. The absorbance values were used to quantify the extent of deprotonation. The pK_a value was interpolated from the fitted sigmoidal (Boltzman) curve as pH corresponding to 1/2 of the total increase of the absorbance due to the deprotonation.

Table 2
Analysis of spectrophotometric titration and fluorescence quenching experiments

Peptide	pK_a [a]	Stern–Volmer quenching constant [b], K_D (M^{-1})	
		I^-	HPO_4^{2-}
Biphalin	9.89 ± 0.01	5.00 ± 0.03	2.91 ± 0.03
Leu–enkephalin	9.96 ± 0.01	4.51 ± 0.03	2.61 ± 0.05
Tyr–D-Ala–Gly	9.97 ± 0.01	6.86 ± 0.10	3.40 ± 0.04

Fluorescence quenching experiment was performed by adding 1 M iodide or 2 M hypophosphate quencher stock solution to obtain quencher concentration between 10 and 200 mM. In spectrophotometric titrations, the pH was varied by adding concentrated NaOH.

[a] The pK_a values were obtained by fitting a sigmoidal (Boltzman) curve to the experimental data points. The reported experimental error reflects the quality of the fitting procedure. However, considering experimental uncertainties due to the sample concentration, we estimate the experimental error as ± 0.1.

[b] The Stern–Volmer constants were obtained by linear regression. The raw data were corrected for the sample dilution due to the added quencher in the experiment.

able to analyze the ratio of the deprotonated-to-protonated tyrosine absorbance, A_{290}/A_{275}, in order to eliminate errors due to sample concentration changes. However, the spectral shape change in the region adjacent to 275 nm observed for biphalin precluded this approach (Fig. 5); instead the absorbance was analyzed using the deprotonated form of tyrosine, centered at 290 nm. Considering the steep absorbance vs. pH dependence (approximately $\Delta A_{290}/\Delta pH = 0.1$) and the dilution of $< 5\%$ of the initial volume, the resulting experimental uncertainty is about 0.1 pH.

Titration of biphalin results in different spectral changes below 275 nm (the wavelength of L_b transition of tyrosine) as compared to both Tyr–D-Ala–Gly and Leu–enkephalin (Fig. 5). The band centered at

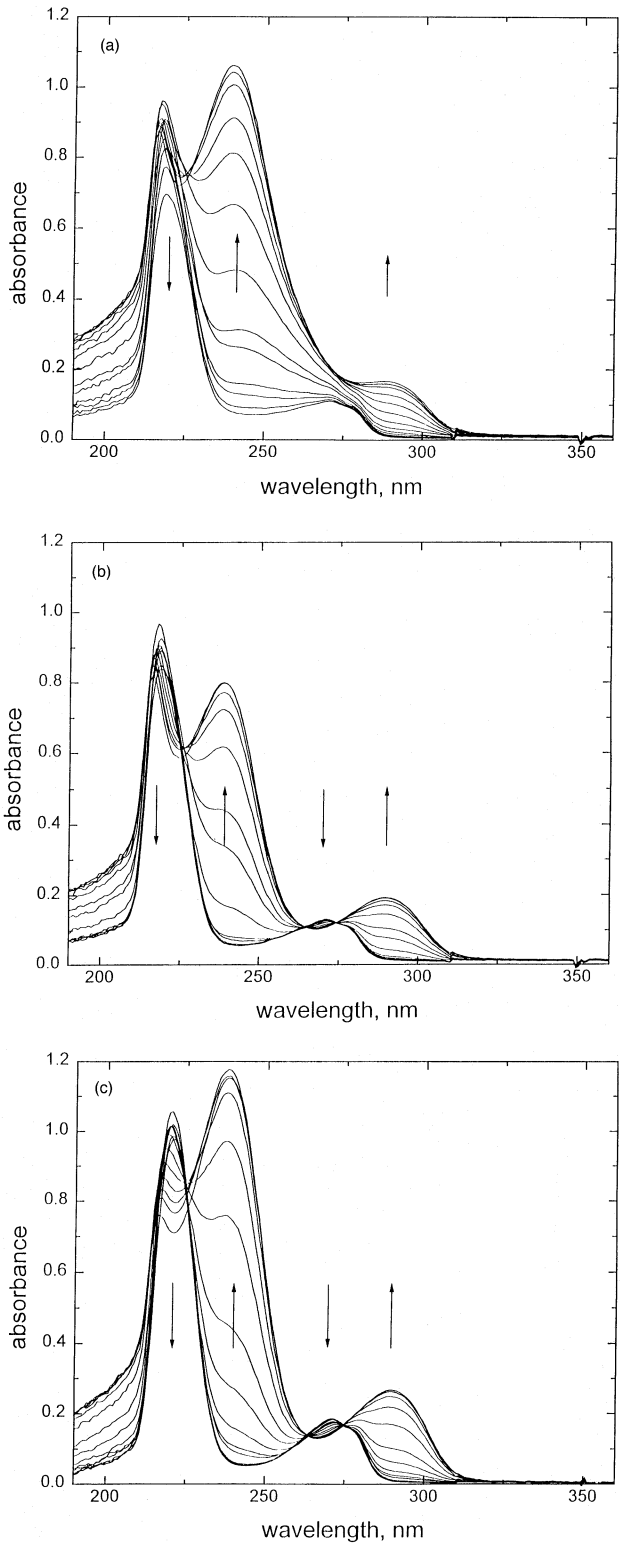

Fig. 5. Absorption spectra of (a) biphalin, (b) Leu–enkephalin, and (c) Tyr–D-Ala–Gly at increasing pH values, from 7.4 to 11.8. Arrows indicate direction of spectral changes due to the increased pH value. Ca. 0.1 mM unbuffered solution of each peptide was titrated using NaOH. The emerging band at 290 nm is used for quantitative analysis of the deprotonated form of tyrosine. The spectral shape of biphalin at higher pH interferes with a reliable determination of absorbance at 275 nm characteristic of the protonated tyrosine.

238 nm, present in both deprotonated Tyr–D-Ala–Gly and Leu–enkephalin, is much stronger, broader and red shifted in biphalin. Analysis of the high pH spectra of these peptides shows that this broad absorption band found for biphalin can be separated into that present in Tyr–D-Ala–Gly or Leu–enkephalin, centered at 238 nm, and an additional band centered at 246 nm (Fig. 6). This relatively strong band changed the appearance of the biphalin spectra at higher pH, as compared to the other peptides studied (Fig. 5), and interfered with the determination of the absorbance of the protonated form of tyrosine at 275 nm. This band is tentatively attributed to the hydrazide bridge of biphalin.

The quenching of tyrosine fluorescence by iodide and phosphate anions was also analyzed (Fig. 7). Quenching measurements can reveal accessibility of fluorophores to quenchers [29]. Fluorescence quenching by iodide is probably a result of intersystem crossing to a weakly luminescent excited triplet state. This intersystem crossing is promoted by spin-orbit coupling within the phenolic ring which is enhanced by the presence of iodide [30]. The proposed mechanism of the tyrosine quenching by phosphate ions involves formation of a hydrogen bond between the hydroxyl group of the excited state tyrosine and the phosphate anion: $-OH\ldots OP(O^-)_2(OH)$ [31]. The tyrosine side chain appears to be less accessible in biphalin or Leu–enkephalin than in the model peptide, Tyr–D-Ala–Gly (Table 2). The Stern–Volmer constants for biphalin or Leu–enkephalin fluorescence quenching are lower than that obtained for the Tyr–D-Ala–Gly model peptide. With all three peptides, the I^- quenching is more efficient than HPO_4^{2-}.

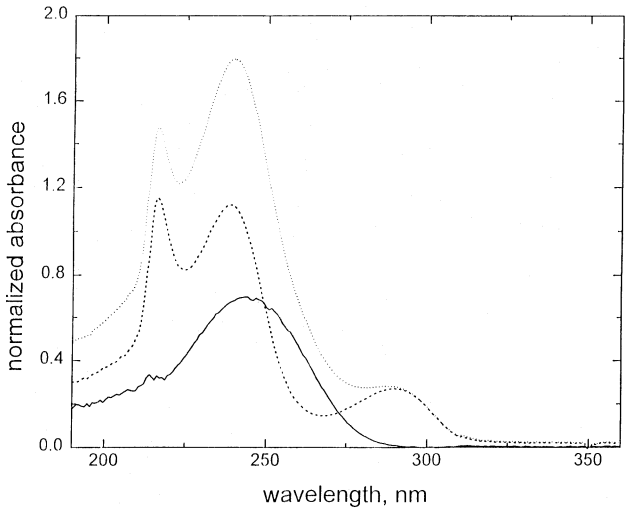

Fig. 6. Analysis of absorption spectra of the tyrosine containing peptides at high pH values (ca. pH 11.5), above the pK_a of the tyrosine hydroxyl group. Absorption spectrum of biphalin (dashed line), Leu–enkephalin (dotted line), and the difference (solid line) are shown. The differential spectrum represents a band centered at 246 nm, characteristic of biphalin but not Leu–enkephalin or Tyr–D-Ala–Gly.

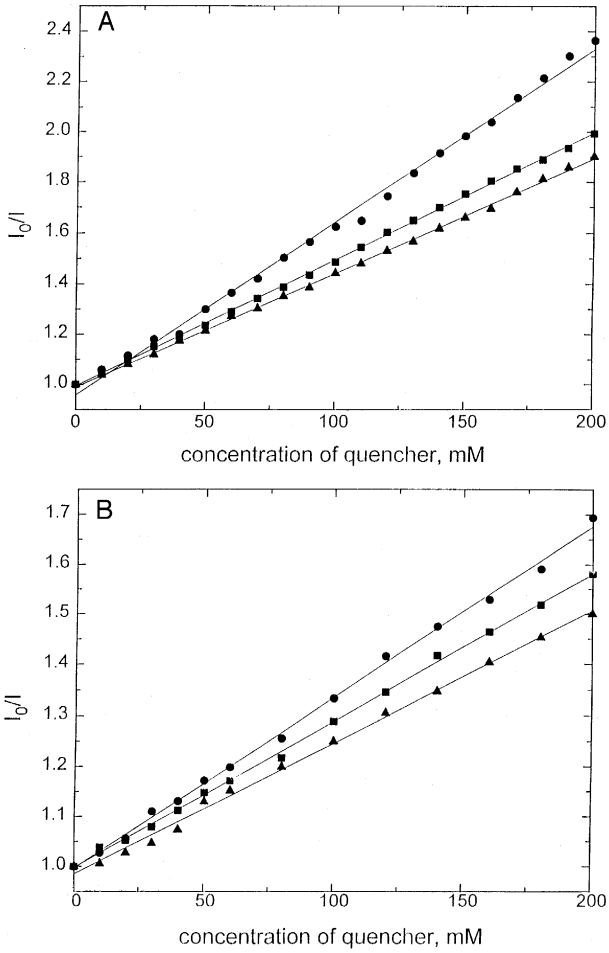

Fig. 7. Iodide (A) and hypophosphate (B) quenching of fluorescence of biphalin (■), Leu–enkephalin (▲) and Tyr–D-Ala–Gly (●). The linear Stern–Volmer plots were obtained based on the intensity of fluorescence excited at 275 nm and detected at 305 nm. The concentration of peptides did not exceed 0.1 mM. The fluorescence of Tyr–D-Ala–Gly is quenched more efficiently than that of Leu–enkephalin or biphalin.

4. Discussion

Our interest in the interaction of different biphalin analogs with model membranes was prompted by our

initial observation that the transfer of biphalins from aqueous phase to model membranes is driven by enthapy change rather than the entropy changes characteristic of the hydrophobic effect [32]. In that experiment, a lipid vesicle suspension was titrated into a solution of [*p*-Cl-Phe$^{4,4'}$]-biphalin, one of the more permeable biphalin analogues. In fact, we found that the overall interaction between the peptide and membrane was exothermic, therefore driven mostly by enthalpy changes, rather than an entropy increase. Previously, we analyzed a series of conformationally restricted cyclic[D-Pen^2,D-Pen^5]-enkephalin analogues modified on the position 3 by increasingly hydrophobic side chains Gly^3 → Ala^3 → Abu^3 → Phe^3 [33]. In that series, we observed that the increasing permeability coefficient depends linearly on the hydrophobicity of the substituted side chains [33], and that indeed the peptide–membrane interaction was entropy driven [32,34]. Furthermore, the permeability of more flexible, but larger octapeptide, i.e. biphalin, is greater than that of the pentapeptide cyclic[D-Pen^2,D-Pen^5]-enkephalin [33]. Thus, the mechanism of transmembrane permeation of flexible biphalins differs substantially from that of conformationally restricted peptides.

Differential scanning calorimetry demonstrates that the interaction between biphalins and lipid molecules within a membrane is rather weak. It is evident that at the peptide-to-lipid molar ratios used in the permeability assays and equilibrium dialysis experiments, not exceeding 1:20, the presence of peptides does not affect the phase behavior of lipid membranes (Fig. 3). This is similar to the observation of Ramaswami et al. [16,33] concerning the interaction of cyclic[D-Pen^2,D-Pen^5]-enkephalin analogues with the same type of model membranes. The observation that the lipid membrane is essentially unperturbed upon the peptide entering membrane supports the passive diffusion model of the transmembrane movement of these agents [3]. According to this model, the observed permeation coefficient is a product of the water–membrane partition coefficient and transmembrane component of the diffusion constant. The measured values of the permeation and partition coefficients (Table 1) are well correlated, both being lower for electron withdrawing substitutions and higher for the electron donating substitutions as compared to the parent compound, biphalin. To understand how the biphalin structure and its modifications control the observed partitioning and permeability, we propose that the flexible biphalin can adopt a folded conformation similar to that observed in the Leu–enkephalin trihydrate crystal structure [35,36]. Both peptides have similar amino acid sequence and comparable affinities for the μ- and δ-opioid receptors [14]. The membrane permeability of Leu–enkephalin (Table 1) is similar to that of the reduced acyclic[D-Pen^2,D-Pen^5]-enkephalin [16]. Both of these acyclic peptides are about 40% more permeable than [*p*-F-Phe$^{4,4'}$]-biphalin. To evaluate the folding of biphalin and Leu–enkephalin the accessibility of the aromatic side chains of these peptides, essential for their biological function, was compared by spectroscopic assays. Consequently, we examined whether the type of folding identified for Leu–enkephalin provides a firm basis for explaining the permeability and partitioning of biphalins.

The spectrophotometric titration does not reveal any differences in the solvent accessibility of the hydroxyl group of the tyrosine residues of biphalin, Leu–enkephalin or the Tyr–D-Ala–Gly model peptide. Unlike the pH titration experiment, the fluorescence quenching study indicates different tyrosine side chain accessibilities among the peptides being tested. The Stern–Volmer constants reveal that accessibility of the tyrosine residue in Leu–enkephalin and biphalin is lower than in the Tyr–D-Ala–Gly (Table 2). Analysis of the three dimensional structure of Leu–enkephalin, which is more complete than biphalin, provides some interesting insights into the possible mechanism of quenching. It is accepted that enkephalins in solution exist as an equilibrium of different conformers [36–38]. The three dimensional structures observed for this peptide can be classified as extended [39], type I′ β-turn (single β-turn) [40] and βIII/βI-folded (fused two β-turns) [35]. The βIII/βI-folded structure of Leu–enkephalin trihydrate [35,36], is characterized by almost orthogonal close contact between the Tyr1 and Phe4. The tyrosine and phenylalanine rings form a face-to-edge oriented pair, characterized by the center-to-center distance of 4.99 Å and the angle between the planes 101° (11° different from perpendicular) [35]. In this conformation of Leu–enkephalin, the phenylalanine residue forms a shallow pocket partially limiting solvent accessibility to the tyrosine fluorophore. The

presence of this folding of Leu–enkephalin in the conformational equilibrium in solution will reduce the quenching efficiency as observed experimentally.

It has been shown that the mutual position of the aromatic side chains of tyrosine and phenylalanine is crucial for δ- or μ-receptor selectivity of peptide ligands [41–43]. The analogous δ/μ affinities and sequence similarities of Leu–enkephalin and biphalin indicate that the folded arrangements of the tyrosine–phenylalanine aromatic side chains, which were previously identified in the Leu–enkephalin trihydrate crystal structure and are suggested to be crucial for μ-receptor recognition, are likely to also contribute to the conformational equilibrium of biphalin. The observed changes in cross-membrane permeation and water–membrane partition of biphalins (Table 1) generally correlate with the electron affinities of the groups substituted at the para position of the benzene ring of Phe4 and Phe4′ of biphalin. The permeability coefficient increases in the following order of substituents: p-NO_2 < p-Cl, lowest for the electron withdrawing substitution and largest for π-electron donating substitution. The arrangement of Tyr1 and Phe4 residues of Leu–enkephalin trihydrate crystal closely resembles a typical Tyr–Phe aromatic pair, characterized by a 5.74 Å centroid distance, and a dihedral angle of 57° (23° different from perpendicular), that is known to contribute as much as negative 1–2 kcal mol^{-1} to the stability of a molecule [44]. The geometry of interacting aromatic pairs results from electrostatic interactions between electron clouds of the rings [44,45]. The potential energy favors an edge-to-face orientation because the aromatic H atoms are positively charged and the C atoms are negatively charged with respect to one another. Substituents having π-electron donating character, e.g., p-Cl or p-F will enhance this electrostatically driven aromatic ring interaction, and increase the folded population of these peptides. The opposite can be expected for, p-NO_2. Based on theoretical and experimental considerations, it is accepted that folded (compact) conformers of otherwise flexible short peptides are energetically favorable within a membrane and the presence of such compact structures favors water-to-membrane partitioning of peptides [7,46,47]. Although the single type I′ β-turn motif [40] does not allow close contact of Tyr1 and Phe4 in Leu–enkephalin, two such turns in a molecule having two tyrosines and two phenylalanines, such as the case with biphalin can create a Tyr1 ⇄ Phe4′ or Tyr1′ ⇄ Phe4 pair. This possibility is illustrated in Fig. 8 where two type I′ β-turns [40] are joined by the rigid hydrazide bridge whose conformation is known from the crystallographic analysis of di-L-phenylalanine hydrazide [41].

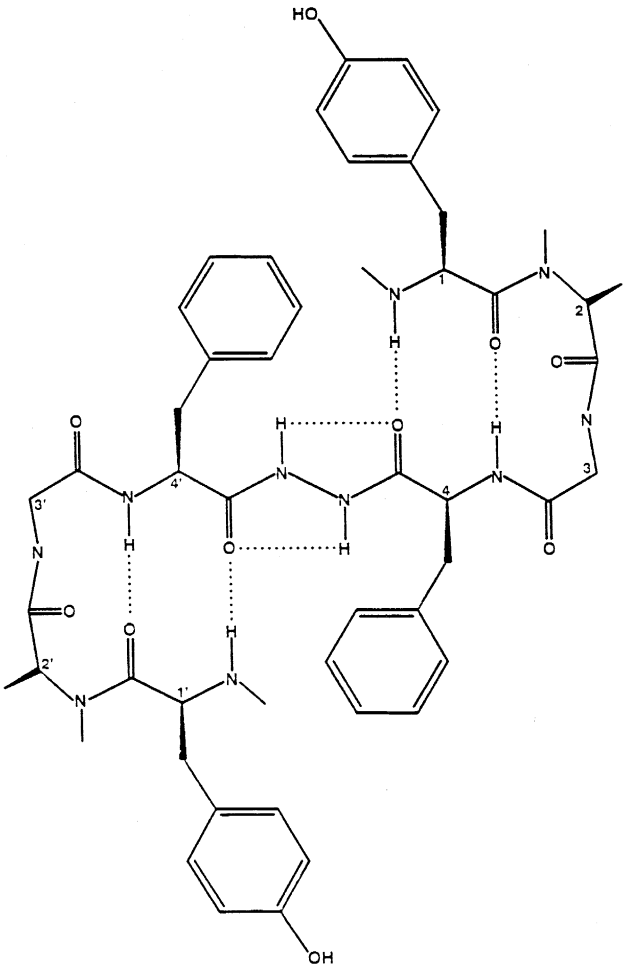

Fig. 8. Folded structure of biphalin. The proposed model comprise two β-turn motifs and a rigid hydrazide bridge. This structure is stabilized by four intramolecular hydrogen bonds, and possibly by formation of aromatic ring pairs, Tyr1–Phe4′ and Tyr1′–Phe4. This specific folding motif explains the chiefly enthalpic character of water-to-lipid transfer of this peptide and the role of different substituents in the para position of phenylalanine in the observed permeability of biphalin analogues (see Section 4).

Our observations emphasize the possible importance of conformational changes that promote the efficient transmembrane movement of biphalins. It

can be anticipated that such changes will be entropically unfavorable, possibly offsetting the hydrophobic effect. A relatively low entropic gain may be characteristic of water-to-membrane partitioning of small peptides that do not posses a stable conformation in water, and have to fold in order to enter a membrane. Among all compact conformers of that peptide, those that minimize the number of hydrogen bonds with water will enter the membrane most efficiently. Although it is well recognized that folding of large peptides facilitates their membrane association, the application of this principle to small peptides appears to useful for enhancing the membrane permeability of these important molecules. In the case of biphalins studied here, the selection of substituents that favor the formation of folded conformations enhanced the permeability by an order of magnitude.

Acknowledgements

This work was supported by NIDA Grant DA 06284.

References

[1] W.D. Stein, Transport and Diffusion Across Cell Membranes, Academic Press, San Diego, CA, 1986, 685 pp.
[2] R.B. Gennis, Biomembranes: Molecular Structure and Function. Springer-Verlag, New York, 1989, 533 pp.
[3] J.M. Diamond, Y. Katz, J. Membrane Biol. 17 (1974) 121–154.
[4] Y. Nozaki, C. Tanford, J. Biol. Chem. 246 (1971) 2211–2217.
[5] C. Chothia, Nature 246 (1974) 338–339.
[6] A. Walter, J. Gutknecht, J. Membrane Biol. 90 (1986) 207–217.
[7] F. Jähnig, Proc. Natl. Acad. Sci. USA 80 (1983) 3691–3695.
[8] L.R. De Young, K. Dill, Biochemistry 27 (1988) 5281–5289.
[9] R.E. Jacobs, S.H. White, Biochemistry 28 (1989) 3421–3437.
[10] W.C. Wimley, S.H. White, Biochemistry 32 (1993) 6307–6312.
[11] W.M. Partridge, Peptide Drug Delivery to Brain, Raven Press, New York, 1991, 357 pp.
[12] A.W. Lipkowski, A.M. Konecka, I. Sroczynska, Peptides 3 (1982) 697–700.
[13] P.J. Horan, A. Mattia, E. Bilsky, S. Weber, T.P. Davis, H.I. Yamamura, E. Malatynska, S.M. Appleyard, J. Slaninowa, A. Misicka, A.W. Lipkowski, V.J. Hruby, F. Porecca, J. Pharmacol. Exp. Ther. 265 (1993) 1446–1454.
[14] A. Misicka, A.W. Lipkowski, R. Horvath, P. Davis, F. Porreca, H.I. Yamamura, V.J. Hruby, Regulatory Peptides 1994 (1994) S131–S132.
[15] T.J. Abbruscato, S.A. Williams, A. Misicka, A.W. Lipkowski, V.J. Hruby, T.P. Davis, J. Pharmacol. Exp. Ther. 276 (1996) 1049–1057.
[16] V. Ramaswami, R.C. Haaseth, T.O. Matsunaga, V.J. Hruby, D.F. O'Brien, Biochim. Biophys. Acta 1109 (1992) 195–202.
[17] M.J. Hope, M.B. Bally, G. Webb, P.R. Cullis, Biochim. Biophys. Acta 812 (1985) 55–65.
[18] S. Udenfriend, S. Stein, P. Bohlen, W. Dairman, W. Leimgruber, M. Weigele, Science 178 (1972) 871–872.
[19] S.M. Johnson, A.D. Bangham, Biochim. Biophys. Acta 193 (1969) 82–91.
[20] S. Kölchens, V. Ramaswami, J. Birgenheier, L. Nett, D.F. O'Brien, Chem. Phys. Lipids 65 (1993) 1–10.
[21] J.C.M. Stewart, Anal. Biochem. 104 (1980) 10–14.
[22] P.J. Clapp, B. Armitage, P. Rossa, D.F. O'Brien, J. Am. Chem. Soc. 116 (1994) 9166–9173.
[23] P.F.F. Almeida, W.L.C. Vaz, T.E. Thompson, Biochemistry 31 (1992) 6739–6747.
[24] P.F.F. Almeida, W.L.C. Vaz, T.E. Thompson, Biophys. J. 64 (1993) 399–412.
[25] R.N.A.H. Lewis, D.A. Mannock, R.N. McElhaney, D.C. Turner, S.M. Gruner, Biochemistry 28 (1989) 541–548.
[26] S. Udenfriend, S. Stein, In: M.A. Lipton, A. DiMascio, K.F. Killam (Eds.), Psychopharmacology: A Generation of Progress, Raven Press, New York, NY, 1978, pp. 459–463.
[27] C.R. Cantor, P.R. Schimmel, Biophysical Chemistry. Part II. Freeman, New York, 1980, 846 pp.
[28] M.A. Spirtes, R.W. Schwartz, W.L. Mattice, D.H. Coy, Biochim. Biophys. Res. Comm. 81 (1978) 602–609.
[29] J.R. Lakowicz, Principles of Fluorescence Spectroscopy, Plenum Press, New York, 1983, 496 pp.
[30] M. Kasha, J. Chem. Phys. 20 (1952) 71–74.
[31] H. Pal, D.K. Palit, T. Mukherjee, J.P. Mittal, J. Photochem. Photobiol. A 52 (1992) 391–409.
[32] M. Romanowski, X. Zhu, A.W. Lipkowski, A. Misicka, R.C. Haaseth, V.J. Hruby, D.F. O'Brien, Biophys. J. 66 (1994) A57.
[33] V. Ramaswami, X. Zhu, M. Romanowski, R.C. Haaseth, A. Misicka, A.W. Lipkowski, V.J. Hruby, D.F. O'Brien, Int. J. Peptide Protein Res. 48 (1996) 87–94.
[34] M. Romanowski, X. Zhu, V.J. Hruby, D.F. O'Brien, Biophys. J. 68 (1995) A441.
[35] A. Aubry, N. Birlirakis, M. Sakarellos-Daitsiotis, C. Sakarellos, M. Marraud, Biopolymers 28 (1989) 27–40.
[36] R. Wiest, V. Pichon-Pesme, M. Bernard, C. Lecomte, J. Phys. Chem. 98 (1994) 1351–1362.
[37] P.W. Schiller, In: S. Udenfriend, J. Meienhofer (Eds.), The Peptides: Analysis, Synthesis, Biology, Vol. 6, Academic Press, Orlando, FL, 1984, pp. 219–268.
[38] W.F. DeGrado, Adv. Protein Chem. 39 (1988) 51–124.
[39] A. Camerman, D. Mastropaolo, I.L. Karle, N. Camerman, Nature 306 (1983) 447–450.

[40] G.D. Smith, J.F. Griffin, Science 199 (1978) 1214–1216.
[41] Z. Urbanczyk-Lipkowska, J.W. Krajewski, P. Gluzinski, A.W. Lipkowski, G. Argay, J. Mol. Struct. 140 (1986) 151–157.
[42] V.J. Hruby, H.I. Yamamura, F. Porreca, Ann. NY Acad. Sci. 757 (1995) 7–22.
[43] X. Qian, K.E. Kövér, M.D. Shenderovich, A. Misicka, T. Zalewska, R. Horvath, P. Davis, F. Porecca, H.F. Yamamura, V.J. Hruby, J. Med. Chem. 37 (1994) 1746–1757.
[44] S.K. Burley, G.A. Petsko, Science 229 (1985) 23–28.
[45] D.A. Dougherty, Science 271 (1996) 163–168.
[46] A.S. Ito, A.M.L. de Castrucci, V.J. Hruby, M.E. Hadley, D. Krajcarski, A.G. Szabo, Biochemistry 32 (1993) 12264–12272.
[47] R.A. Gray, D.G. Vander Velde, C.J. Burke, M.C. Manning, C.R. Middaugh, R.T. Borchardt, Biochemistry 33 (1994) 1323–1331.